Polymer Nanoparticle Superlattices for Organic Photovoltaic Applications

ARTICLE *in* JOURNAL OF PHYSICAL CHEMISTRY LETTERS · DECEMBER 2011

Impact Factor: 7.46 · DOI: 10.1021/jz2012275

8 AUTHORS, INCLUDING:

Mina Baghgar

15 PUBLICATIONS **154** CITATIONS

SEE PROFILE

Ying Yang

Keele University

1,422 PUBLICATIONS **30,297** CITATIONS

SEE PROFILE

Dhandapani Venkataraman

University of Massachusetts Amherst

114 PUBLICATIONS **4,366** CITATIONS

SEE PROFILE

Michael D Barnes

University of Massachusetts Amherst

147 PUBLICATIONS **2,326** CITATIONS

SEE PROFILE

THE JOURNAL OF PHYSICAL CHEMISTRY Letters

PERSPECTIVE

pubs.acs.org/JPCL

Polymer Nanoparticle Superlattices for Organic Photovoltaic Applications

Joelle A. Labastide,[†] Mina Baghgar,[‡] Irene Dujovne,[†] Yipeng Yang,[‡] Anthony D. Dinsmore,[‡] Bobby G. Sumpter,[§] Dhandapani Venkataraman,[*,†] and Michael D. Barnes[*,†,‡]

[†]Department of Chemistry, University of Massachusetts Amherst, 710 North Pleasant Street, Amherst, Massachusetts 01003, United States

[‡]Department of Physics, University of Massachusetts Amherst, 666 North Pleasant Street, Amherst, Massachusetts 01003, United States

[§]Computer Science and Mathematics Division, and Center for Nanophase Materials Sciences, Oak Ridge National Laboratory, Oak Ridge, Tennessee 37831, United States

ABSTRACT: In this Perspective, we discuss the possibility of constructing binary nanoparticle superlattices for organic photovoltaic applications and some of the interesting new photophysics emerging from preliminary studies. We summarize recent advances in nanoparticle preparation and photophysical characterization and some of the very interesting observed departures from thin-film photoluminescence dynamics. We conclude by discussing some of the challenges ahead and the possibility of new emergent physics in the assembly of polymer nanoparticles into functional devices.

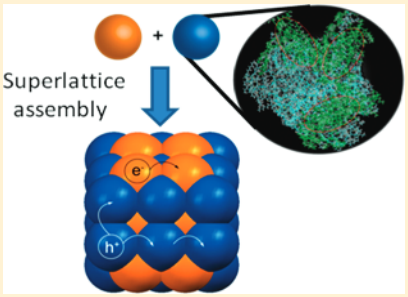

Semiconducting Polymer Nanoparticles As Building Blocks for Organic Photovoltaics. In the past several years, there has been an explosion of research aimed ultimately at solar energy harvesting devices built from cheaply processable organic semiconductors with efficiencies rivaling or surpassing those of inorganic systems. One of the main roadblocks is the issue of exciton diffusion length. For inorganic semiconductors, in particular indirect band gap materials such as silicon, this distance can be on the order of tens of micrometers, while for direct band gap organic materials, this distance is ~10 nm. Thus, significant effort has been focused on engineering polymer domain dimensions in this size range to facilitate efficient separation of photogenerated electrons and holes. Of course, this is only one aspect of a very complicated problem.[1] To succeed in the development of high-efficiency organic photovoltaic (OPV) systems, one also needs to construct continuous conduction paths to the cathode and anode to avoid simply generating charge traps and subsequent material degradation. In this Perspective, we discuss the possibility of nanoparticle superlattices for organic photovoltaic applications and some of the interesting new photophysics that are emerging from our preliminary studies.

Figure 1 illustrates the basic concept of our approach. We envision organization of the n-type (electron-rich) and p-type (electron-poor) moieties into separate approximately spherical nanoparticles and then organizing the nanoparticles into stable superlattices whose crystalline structure is defined by the nanoparticle radii. In 1929, Pauling formally enunciated the radius ratio (R_{cation}/R_{anion}) rules for predicting the coordination number and thus the structures of ionic crystals.[2] Akin to the formation of binary ionic crystals, two types of nanoparticles

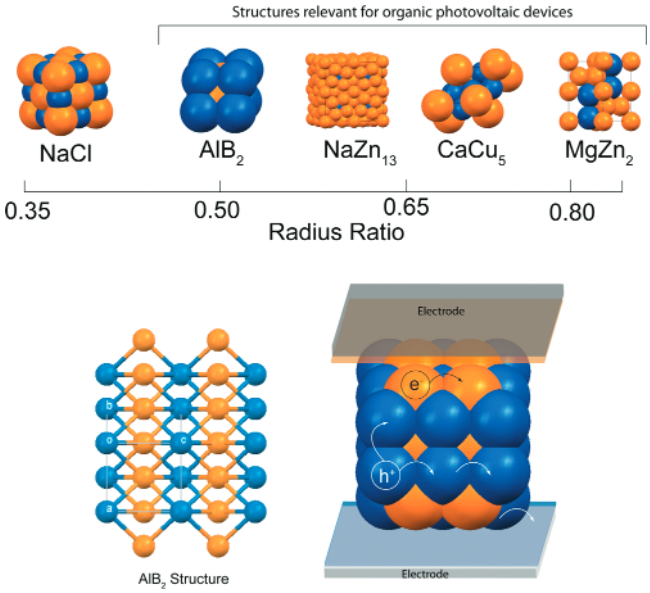

Figure 1. (Top) Superlattice crystal structures obtained by the assembly of nanoparticles with a specific radius ratio. (Bottom) Expanded view of the AlB2 structure showing continuous pathways for electron/hole transport to the anode/cathode, respectively.

Received: September 8, 2011
Accepted: November 16, 2011
Published: November 16, 2011

dx.doi.org/10.1021/jz2012275 | *J. Phys. Chem. Lett.* 2011, 2, 3085–3091

can also self-assemble into ordered "superlattices".[3−5] As in the ionic crystal case, the packing of the nanoparticles also depends on the ratio of the radii of the particles ($\gamma = R_{small}/R_{large}$), and the self-assembly of nanoparticle mixtures occurs even if the nanoparticles have interactions different from Coulomb's law.[5,6] This approach potentially changes the paradigm for forming semiconductor assemblies and allows considerable flexibility in the nanoscale architecture. While the formation of a variety of binary lattices has been found using micrometer-sized polymer spheres, reports on the self-assembly of nanoparticles are limited to inorganic nanoparticles (quantum dots). We believe that the concept of packing nanoparticles is a powerful tool to reliably obtain stable structures relevant for solar energy conversion, and the concept of binary nanoparticle self-assembly should be extended to π-conjugated organic and polymer systems. The packing of individual polymer chains within the nanoparticles can ultimately be optimized with respect to charge mobility by annealing the particles prior to assembly. At the same time, the characteristic length scale (lattice constant of the nanoparticle assembly) in the composite superlattice can ultimately be tuned to match the exciton diffusion length by changing the radii of the particles. Hence, the particle packing approach offers the potential to optimize the structure independently at the molecular and nanometer scales.

The ultimate goal, and significant challenge, is to prepare assemblies of particles that result in continuous but separate conduction paths for electrons and holes.

The ultimate goal, and significant challenge, is to prepare assemblies of particles that result in continuous but separate conduction paths for electrons and holes. As shown in Figure 1, the AlB_2 structure consisting of alternating layers of Al and B atoms represents one family of structures that would facilitate extended continuous pathways for charge transport. This same structure type (but at a larger scale) has been obtained by self-assembly of 6.7 nm nanoparticles of PbS and 3 -nm nanoparticles of Pd.[3] Now, consider the possibility of replacing the PbS and Pd nanoparticles in the AlB_2 structure with electron-conducting and hole-conducting organic nanoparticles. The resultant assembly will effectively have a lamellar arrangement of semiconductors, that is, alternating layers of hole and electron conductors, the most widely targeted structure for bulk heterojunction OPV cells (Figure 1, bottom right). Similarly, if nanoparticles were arranged with the same structure as the minerals $CaCu_5$ and $MgZn_2$, there would again be continuous conduction pathways through each species of nanoparticles with an interface between the two pathways. By contrast, the NaCl structure ($\gamma \approx 0.35$) would not provide a conduction pathway for both electrons and holes because the smaller (blue) spheres do not percolate (Figure 1). By varying the radius ratio of the particles and the solvent-induced interactions between particles, it should be possible to tune the packing geometry to obtain different structure types and evaluate their potential for OPV devices. Among the possibilities listed in Figure 1, the AlB_2, $CaCu_5$, and $MgZn_2$ structure types are of key interest as they can result in continuous conduction paths for photogenerated charges.

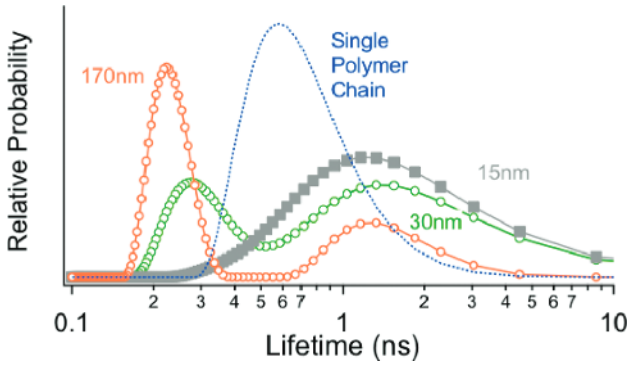

Figure 2. Fluorescence lifetime probability distribution functions obtained by regularized Laplace inversion of the measured PL decay data. The prompt component ($t \approx 250$ ps) appears to be associated with the crystalline composition of the nanoparticle.

Polymer Nanoparticle Preparation. There are several different ways to prepare polymer nanoparticles. Nebulization or microdroplet techniques have been used to generate highly monodisperse polymer and polymer blend particles.[7,8] However, because the particle production rate is defined by the frequency of the droplet generator, it is often difficult to obtain high sample throughput using microdroplet approaches. With a vibrating orifice aerosol generator (VOAG), the size dispersity of the initial solvent droplets can be quite small (<1 part in 10^5, depending on the initial droplet size, which ranges from 25 to ~100 μm); however, subtleties arise when considering final nanoparticle size and size dispersity associated with Poisson occupation statistics. For example, if the target size is ≤10 nm, the maximum number of polymer chains that can pack into a nanoparticle of that size is ~15, assuming an average molecular weight of 5×10^4 g/mol (typical of commercially available rr-P3HT). Assuming Poisson occupation statistics, the ultimate uncertainty in diameter (proportional to $N^{1/3}$, where N is the number of polymer chains) would be ~10%. By reducing the average molecular weight by a factor of 2, the Poisson limit in the nanoparticle size dispersity is ~6%. In addition, as pointed out in a recent paper, regioregularity plays an important role in molecular packing.[9]

Polymer nanoparticles are also readily prepared using miniemulsion techniques.[10,11] Accessible to a broad range of polymeric systems, these techniques work either by polymerization of the monomer within micro- or nanoscopic liquid droplets (miniemulsion polymerization) or by postpolymerization dispersion of the polymer into droplets, followed by removal of the droplet-phase solvent.[10,11] The latter approach provides separate control of the polymerization and particle formation processes and is compatible with a wide variety of polymer and oligomeric systems. In either approach, the size polydispersity tends to be broad, at least several percent of the mean diameter, which is attributed to the polydispersity in the miniemulsion droplet sizes.[12,13] To date, the nanoparticle size dispersity reported in the literature appears to be too large to allow long-range crystalline order in superlattices. This observation stands in contrast to inorganic nanoparticles, which can be made very monodisperse and which can form very ordered superlattices (as described

elsewhere in this Perspective). In the polymer case, the miniemulsion route might yield a more uniform size distribution if existing techniques were used to narrow the droplet size distribution in the early stage of nanoparticle formation.[13,14]

We have prepared polythiophene nanoparticles as small as 15 nm using a miniemulsion technique and commercially available rr-P3HT polymer. Briefly, this is accomplished by first preparing a surfactant solution (e.g., sodium dodecyl sulfate, SDS) in distilled water; the final mean nanoparticle size appears to be most sensitive to the surfactant concentration and initial concentration of the polymer solution. Then, a definite volume of dilute polymer solution in a 'good' solvent (e.g., $CHCl_3$ for polythiophene) is injected into the surfactant solution. The mixture is typically sonicated in an ultrasound bath for ~2 min and then heated directly on a hot bath with a surface temperature of ~125 °C until all of the chloroform has evaporated. The end result is a dispersed suspension of surfactant-capped polymer nanoparticles in water. We typically characterize the polymer nanoparticle size (and size dispersity) by solution-phase dynamic light scattering (DLS) and in situ atomic force microscopy. Of particular interest is the volume fraction of crystalline polythiophene in the nanoparticles as this is directly relevant to charge-separation efficiency. The volume fraction of crystalline polymer within the nanoparticle was estimated, using the empirical rule proposed in the literature, by the relative intensity of the shoulder peak at 600 nm with respect to λ_{max} in the absorption spectrum.[15] The smallest nanoparticles that we have been able to prepare reproducibly have a mean size of ~15 nm with a size dispersity of about 15%. This size is suitable to obtain a bicontinuous structure with a characteristic length scale close to the exciton diffusion length, but more work is needed to approach the 5−7% size dispersity required for crystalline superlattice formation.

Size-Dependent NP Photophysics. Unlike their inorganic counterparts, polymer nanoparticles are generally not expected to show any distinct size-dependent electronic behavior associated with charge delocalization. In aggregated polymer systems, effects of interchain coupling are typically manifested as a red-shifted spectral component due to H- or J-aggregate formation.[16,17] Studies of multichain aggregates of poly(phenylene-vinylene) (PPV) systems, for example, typically show significant luminescence quenching, associated with carrier trapping at interchain boundaries and defects.[18,19] In contrast with PPVs, polythiophenes (PTs) are a class of semiconducting polymers that have been designed to crystallize; the photophysics of semicrystalline polythiophene and polythiophene blends are significantly more complex and are currently the focus of intense research efforts across many different disciplines.[20−26] The competition between charge separation and recombination in semicrystalline polythiophene is, of course, good news for photovoltaic applications. At the same time, charge separation makes many of the optical studies, which have proven so fruitful for PPVs, problematic due to significantly reduced photoluminescence (PL) count rates, combined with very fast (<100 ps) and very slow (>10 ns) recombination processes.

In our initial investigations of isolated P3HT nanoparticle photophysics, we have observed several intriguing size-dependent features in the single-particle photoluminescence that are connected with exciton diffusion and dissociation dynamics.

In our initial investigations of isolated P3HT nanoparticle photophysics, we have observed several intriguing size-dependent features in the single-particle photoluminescence that are connected with exciton diffusion and dissociation dynamics. [27] Our experimental approach was to use a variant of time-tagged/time-resolved (T3R) photon counting, in which a polarization "tag" for each detected photon is also recorded. This allows access to polarization contrast information on subnanosecond time scales and the time evolution (with time resolution defined ultimately by the time-to-digital converter) of PL polarization from the first 10 ps to hundreds of nanoseconds, depending on the photostability. Measurements of the time evolution of polarization contrast show an interesting size dependence that appears to be also related to the volume fraction of crystalline P3HT within the nanoparticle.[27]

Figure 2 summarizes the trend in PL decay dynamics with nanoparticle size, representing the PL decay function as a decay rate probability distribution obtained from a regularized fit to the data using a discrete grid of decay rate (time constant) points.[28−30] For every nanoparticle size family studied, the PL decay was nonexponential, while for single P3HT polymer chains (cast from chloroform), the PL decay was approximately single-exponential with a characteristic lifetime of ~600 ps. For 15 nm particles, the PL decay appeared significantly longer than that of a single chain, with a broad (approximately continuous) lifetime distribution ranging from 200 ps to 6 ns. For the larger sizes, the PL decay rate distribution became increasingly bimodal with a prominent fast decay component and a lifetime of ~250 ps.

In addition to the short-time behavior, we also observed some very interesting size-dependent differences in PL decay at long times. In the 10−100 ns time regime, the PL originates not from radiative transitions of bound excitons but rather from charge separation followed by bipolaron recombination and thus provides an interesting measure of exciton fission probability within the nanoparticle.[26,31] A distinct signature of bipolaron recombination is a power law decay (proportional to $t^{-(1+\mu)}$) where the power law exponent μ is a tunneling width parameter divided by a mean electron−hole separation distance.[26] Power law behavior in the charge-carrier density in polythiophene films has been extensively studied using both optical[26] and magnetic resonance approaches.[32−34] For larger nanoparticles (>120 nm), we recovered a value of $\mu \approx 0.7$, which is close to the reported thin-film value of 0.54.[26] For smaller particles, we observed an increase in the power law exponent with decreasing particle size ($\mu \approx 1.4$ for 60 nm particles),[27] suggesting a decrease in the average electron−hole radius resulting from smaller crystalline domains within the nanoparticles. The internal structure figures of merit—domain size and degree of polycrystallinity—appear to depend on nanoparticle size and are signaled by different temporal and polarization properties of the PL.

Theoretical Challenges. There is a large body of primarily anecdotal information on the different morphologies needed to

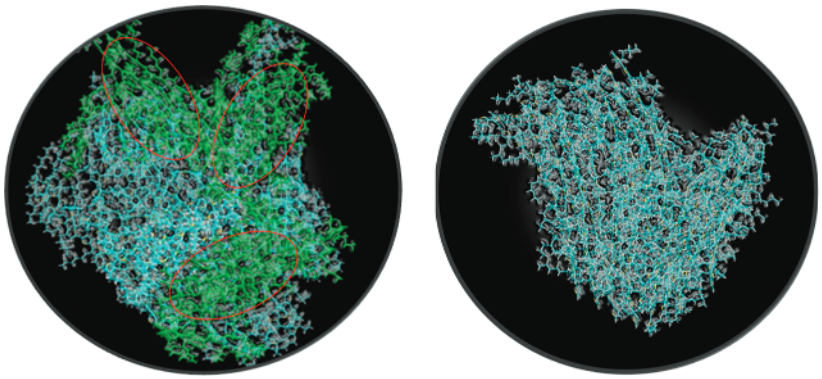

Figure 3. (Left) Structure of a P3HT nanoparticle (~10 nm diameter) composed of regioregular P3HT chains with 12 monomers. (Right) A ~4 nm particle created using the same simulation protocol showing primarily only one "wire" domain. The results were obtained from classical molecular dynamics simulations of a P3HT system consisting of 120 chains (room-temperature dynamics over 18 ns followed by molecular mechanics minimization). The green highlighted and circled regions show P3HT chains ordered into π-stacked crystalline domains (size of 1−2 nm) with no particular orientational ordering.

improve the power conversion efficiency in organic photovoltaic systems but far less information on fundamentally applicable design parameters based on theoretical modeling.[1] Many of the interesting photophysical properties of thiophenes derive from low-lying triplet states that are accessible from singlet fission, provided that there is a proper alignment of the electronic states.[35,36] These low-lying states can thereby generate longer-lived excitonic or polaronic states that improve charge extraction efficiency. However, these photophysical processes also add considerable complexity to the problem of understanding electronic processes in P3HT-based materials. In fact, accurate mapping of structure−property−transport relationships for these materials in the thin-film morphologies required for use in solar cells has proven very difficult.[37] Even in the single-component case, a detailed understanding of the inherent molecular structure of P3HT and the underlying energy landscape that controls the time-dependent evolution and interfacial structures is needed, one of the most important features being the degree of intermolecular P3HT interactions in the form of interchain $\pi-\pi$ stacking and the orientation of the resultant stacked chain domains relative to the solar cell electrodes (carrier mobility is highest in the π-stacked direction).[38−40]

A bulk heterostructure that percolates throughout the material with multiple ordered/crystalline domains of ~10 nm should, in principle, have good photovoltaic properties. However, in such a material, the nature of interfacial interactions between the donor and acceptor domains becomes critical as even small changes in the orientation of a P3HT chain relative to an acceptor like PCBM can drastically decrease charge-transfer efficiencies. Similar complexities arise at additional interfaces at the electrodes, where it is clear that the inherent material structure and dynamics are modified due to other types of interfacial interactions. Another notable difficulty in the quest to understand structure−property−transport relationships is associated with the effects of rheology, particularly in thin films as a result of solvent spin-casting. Although thermal or solvent annealing can improve reproducibility in optoelectronic response, the spin-cast film is inherently a nonequilibrium system, further complicating development of a detailed theoretical description. Thus, the multicomponent material structure of a general P3HT/PCBM thin film likely presents a dynamic heterogeneity, which is typically believed to be on the 2 nm length scale.

The diversity of physics involved in modeling assembly and electronic processes in organic semiconductor nanoparticles presents significant challenges to existing computational algorithms and capabilities.

The diversity of physics involved in modeling assembly and electronic processes in organic semiconductor nanoparticles presents significant challenges to existing computational algorithms and capabilities (e.g., extended time scales for molecular dynamics, beyond density functional and linear response theory for photophysics and interfacial interactions, and nonadiabatic processes underlying stochastic processes of coupled electron−ion dynamics[41]). Some progress has been reported, for example, in relation to understanding the self-assembly of P3HT chains, where a combination of quantum DFT and molecular dynamics simulations found that P3HT domains can be composed of ordered P3HT chains stacked into a staggered geometry that leads to two-dimensional hydrophobic foil-like structures that subsequently assemble into zigzag bulk structures.[42] This process is altered by the presence of surface interactions, in which case, the P3HT chains favor alignment instead of stacking. There is much remaining work to be done in order to unravel all of the intrinsic processes associated with P3HT thin films and especially multicomponent blends.

Superlattices of polymer nanoparticles offer one possible avenue toward removing some of these complexities. In this case, the material length scale is limited by the size of the nanoparticle, and the underlying structural organization (self-assembly) of the P3HT molecules could potentially be equilibrated, thus removing the effects of rheology described above. Moreover, the structural organization of the P3HT molecules can be suitably determined using molecular dynamics simulations without the approximations introduced by course graining

or ad hoc boundary conditions. Figure 3 illustrates an example of the structure obtained from molecular dynamics simulations for a spherical nanoparticle of ~10 nm as compared to one of 4 nm. The smaller nanoparticle shows primarily one crystalline domain, while the larger particle clearly has multiple domains of liquid-crystalline-like order without any discernible preference for orientation. Preliminary semiempirical quantum calculations for stacks of P3HT chains give a UV−vis absorption spectrum, which shows the signature 600 nm shoulder associated with the $\pi-\pi$ stacking with an intensity that qualitatively agrees with that obtained from the experimental measurements of the different sized particles. This agreement, along with the fact that the simulated smaller nanoparticle is less polycrystalline than the larger, provides evidence to support the thesis of this Perspective.

Particle Assembly. Maximization of entropy is the primary mechanism that drives assembly of spherical particles into crystalline arrays (or superlattices) by adopting the most efficient packing geometry.[43] The classic example of entropy-driven crystallization is the formation of face-centered cubic (FCC) arrays of hard spheres (i.e., particles with billiard-ball-like interactions). The FCC and hexagonal close-packed (HCP) lattices have the largest close-packed particle volume fraction, ϕ_{cp}, of any ordered lattices containing spheres of the same size, $\phi_{cp} = 0.74$. By contrast, a liquid has comparatively inefficient packing, with $\phi_{cp} \approx 0.64$. In a sample of given particle volume fraction ϕ, the amount of free volume per particle is related to $\phi_{cp} - \phi$; hence, the efficiently packed FCC and HCP lattices provide more free volume (and hence entropy) to each particle than does a liquid. Computer simulations,[43] theory,[44−46] and experiments with micrometer-size colloidal spheres show that the same maximum-efficiency packing principle applies in mixtures of two different sizes, in which AlB_2 and AlB_{13} superlattices were found in systems with size ratios γ of approximately 0.58 and 0.62.[47−49] Recent investigations of binary nanoparticle mixtures with $0.57 < \gamma < 0.81$ have found these and other structures.[4] Different equilibrium structures might arise in mixtures of particles having weak enthalpic interactions (arising from electrostatic or van der Waals forces, for example); in these cases, the crystal geometry might not be the one that maximizes ϕ_{cp}. For example, the relatively low packing fraction of $MgZn_2$, $\phi_{cp} = 0.7$, suggests that attractive interactions may favor this structure relative to the formation of two separate FCC lattices.[50] Additional insight has come from experiments with charged nanoparticles, where electrostatic interactions alter the packing structure and increase the diversity of equilibrium structures.[3,51,52] For example, a binary mixture of PbSe nanoparticles with oleic-acid-functionalized Au nanoparticles adopted the CuAu lattice structure, whereas the same particles stabilized with tri-*n*-octylphosphine oxide (TOPO) adopted the $CaCu_5$ lattice. In the former case, electrophoretic mobility measurements showed that the two nanoparticles had opposite charge; in the latter case, the charge was less, and the structure corresponded to the more efficient packing. Experiments with micrometer-scale spheres have covered a wide range of size ratios and indicate that still more structures can be stable when the charge interactions are stronger.[53,54] Hence, the ability to control and measure the surface charge of the nanoparticles will be an important part of a program of directed assembly. In many cases, the mechanism of charging is not well understood, which offers an interesting area of future research.[3,5]

Summary and Outlook. Finally, we identify two key future research challenges that will demand close attention. First,

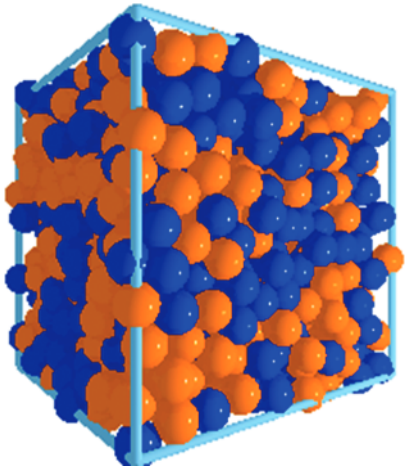

Figure 4. Disordered packing of electron- and hole-transporting polymer nanoparticles with continuous pathways for efficient charge transport.

obtaining crystalline nanoparticle ordering requires a rather narrow distribution of particle sizes for each component,[55] which in turn places stringent demands on synthetic control. This problem might be circumvented by a disordered packing of two different types of polymeric nanoparticles (Figure 4). A disordered packing structure could still provide continuous pathways for electrons and holes and thus be a desirable target for OPV devices. A key part of obtaining a disordered binary structure is to tune the particle sizes and interactions so as to avoid demixing of the particles; this could be a challenge if the two particle sizes are very distinct or if the A−A and B−B interactions are more favorable than the A−B interactions. The second research challenge is to design optimal interfacial interactions between donor (P3HT) and acceptor (PCBM) nanoparticles in the superlattice geometry. One possibility is to utilize semiconducting polymer brushes directly grafted onto the nanoparticle and electrode surfaces.[56] In principle, a suitable density and chain length of tethered P3HT chains can be

A key part of obtaining a disordered binary structure is to tune the particle sizes and interactions so as to avoid demixing of the particles.

prepared such that a deposited nanoparticle superlattice would lead to complete interpenetration/interdigitation and thus formation of a bridging interface with appropriate interactions. To date, there is some preliminary evidence that suggests that such an approach for bulk heterojunction P3HT/PCBM can be fruitful. Computational simulations can be of great utility in this area as the density and chain-length dependence of the interface formed between the donor and acceptor nanoparticle can potentially be mapped out. Additionally, the resultant charge-transfer properties can be examined. The goal is to "rationally" design the donor and acceptor nanoparticles and interfacial ligands.

AUTHOR INFORMATION

Corresponding Author

*E-mail: mdbarnes@chem.umass.edu (M.D.B.); dv@chem.umass.edu (D.V.).

BIOGRAPHIES

Joelle Labastide is a 2nd year chemistry graduate student at University of Massachusetts-Amherst. She received her B.S. in Chemical Engineering from UMass-Amherst in 2010. She is a research assistant in Professor Barnes' group, studying time-resolved photoluminescence in quantum dots and semiconducting polymer nanoparticles.

Mina Baghgar is a 3rd year physics graduate student at University of Massachusetts-Amherst. She received her M.S. in physics from University of Tehran. She is a research assistant in Professor Barnes' group, studying polarization-resolved photoluminescence and near-field optical measurements in quantum dots and semiconducting polymer nanoparticles.

Yipeng Yang is a 5th year physics graduate student at UMass Amherst. He got his B.S. from Univ. of Sci. and Tech. of China in 2007 and M.S. from University of Massachusetts-Amherst in 2010. He is now a Ph.D. candidate in physics and a research assistant in Professor Dinsmore's group.

Irene Dujovne received her Ph.D in Applied Physics with distinction from Columbia University in 2005. She was a postdoctoral fellow with Prof. Cees Dekker at TU Delft from 2005 to 2008. In 2011 she joined the Chemistry Department at University of Massachusetts-Amherst as a Senior Research Fellow.

Anthony Dinsmore received his Ph.D. in Physics from the University of Pennsylvania in 1997. He was then a National Research Council Postdoctoral fellow at the Naval Research Laboratory, then a postdoctoral fellow with Prof. David Weitz at Harvard University. In 2001, he joined the Physics faculty at UMass Amherst. http://people.umass.edu/dinsmore/

Bobby G. Sumpter received his Ph.D. in Physical Chemistry from Oklahoma State University in 1986. Following postdoctoral studies at Cornell University and at the University of Tennessee, he joined the Chemistry Division at Oak Ridge National Laboratory. He is currently the group leader for Computational Chemical and Materials Sciences and the Nanomaterials Theory Institute.

www.csm.ornl.gov/comp_materials/ www.cnms.ornl.gov/people/SUMPTER_Bobby.pdf

D. Venkataraman, aka D.V., is an associate professor of chemistry at the University of Massachusetts Amherst. His current research focuses on the directed assembly of molecules and nanoparticles in the condensed state for efficient charge transport. For further information, see http://thedvgroup.com

Michael D. Barnes received his Ph.D. in Chemistry from Rice University in 1991. He was then a Postdoctoral fellow and Staff Scientist at Oak Ridge National Laboratory. He joined the Chemistry Faculty at the University of Massachusetts-Amherst in 2004, with an adjunct position in the Physics department. His research focuses on single-molecule spectroscopy of nanostructured semiconductors. http://www.chem.umass.edu/faculty/barnes.html

ACKNOWLEDGMENT

This material is based on work supported as part of Polymer-Based Materials for Harvesting Solar Energy, an Energy Frontier Research Center funded by the U.S. Department of Energy, Office of Science, Office of Basic Energy Sciences under Award Number DE-SC0001087. J.A.L. and M.B. acknowledge support from the NSF-MRSEC (DMR-0820506). I.D. and M.D.B. acknowledge support of the U.S. Department of Energy Basic Energy Sciences (DE-FG02-05ER15965). Some of the preliminary computations were performed at the Center for Nanophase Materials Sciences, sponsored by the Scientific User Facilities Division, Office of Basic Energy Sciences, U.S. Department of Energy. The assistance of Aidan McKenna and Austin Barnes for nanoparticle preparation and size characterization is gratefully acknowledged.

REFERENCES

(1) Dang, M. T.; Hirsch, L.; Wantz, G. P3HT:PCBM, Best Seller in Polymer Photovoltaic Research. *Adv. Mater.* **2011**, *23*, 3597–3602.

(2) Pauling, L. The Principles Determining the Structure of Complex Ionic Crystals. *J. Am. Chem. Soc.* **1929**, *51*, 1010–1026.

(3) Shevchenko, E. V.; Talapin, D. V.; Kotov, N. A.; O'Brien, S.; Murray, C. B. Structural Diversity in Binary Nanoparticle Superlattices. *Nature* **2006**, *439*, 55–59.

(4) Chen, Z.; O'Brien, S. Structure Direction of II−VI Semiconductor Quantum Dot Binary Nanoparticle Superlattices by Tuning Radius Ratio. *ACS Nano* **2008**, *2*, 1219–1229.

(5) Talapin, D. V. LEGO Materials. *ACS Nano* **2008**, *2*, 1097–1100.

(6) Eldridge, M. D.; Madden, P. A.; Frenkel, D. Entropy-Driven Formation of a Superlattice in a Hard-Sphere Binary Mixture. *Nature* **1993**, *365*, 35–37.

(7) Kumar, P.; Mehta, A.; Mahurin, S. M.; Dai, S.; Dadmun, M. D.; Sumpter, B. G.; Barnes, M. D. Formation of Oriented Nanostructures from Single Molecules of Conjugated Polymers in Microdroplets of Solution: The Role of Solvent. *Macromolecules* **2004**, *37*, 6132–6140.

(8) Barnes, M. D.; Mehta, A.; Kumar, P.; Sumpter, B. G.; Noid, D. W. Confinement Effects on the Structure and Dynamics of Polymer Systems from the Mesoscale to the Nanoscale. *J. Polym. Sci. Part B: Polym. Phys.* **2005**, *43*, 1571–1590.

(9) Adachi, T.; Brazard, J.; Ono, R. J.; Hanson, B.; Traub, M. C.; Wu, Z.-Q.; Li, Z.; Bolinger, J. C.; Ganesan, V.; Bielawski, C. W.; et al. Regioregularity and Single Polythiophene Chain Conformation. *J. Phys. Chem. Lett.* **2011**, *2*, 1400–1404.

(10) Mecking, S.; Pecher, J. Nanoparticles of Conjugated Polymers. *Chem. Rev.* **2010**, *110*, 6260–6279.

(11) Tuncel, D.; Demir, H. V. Conjugated Polymer Nanoparticles. *Nanoscale* **2010**, *2*, 484–494.

(12) Landfester, K. Polyreactions in Miniemulsions. *Macromol. Rapid Commun.* **2001**, *22*, 896–936.

(13) Landfester, K. The Generation of Nanoparticles in Miniemulsions. *Adv. Mater. (Weinheim, Ger.)* **2001**, *13*, 765–768.

(14) Mason, T. G. New Fundamental Concepts in Emulsion Rheology. *Curr. Opin. Colloid Interface Sci.* **1999**, *4*, 231–238.

(15) Wang, T.; Dunbar, A. D. F.; Staniec, P. A.; Pearson, A. J.; Hopkinson, P. E.; MacDonald, J. E.; Lilliu, S.; Pizzey, C.; Terrill, N. J.; Donald, A. M.; et al. The Development of Nanoscale Morphology in Polymer: Fullerene Photovoltaic Blends during Solvent Casting. *Soft Matter* **2010**, *6*, 4128–4134.

(16) Spano, F. C.; Yamagata, H. Vibronic Coupling in J-Aggregates and Beyond: A Direct Means of Determining the Exciton Coherence Length from the Photoluminescence Spectrum. *J. Phys. Chem. B* **2011**, *115*, 5133–5143.

(17) Spano, F. C. The Spectral Signatures of Frenkel Polarons in H- and J-Aggregates. *Acc. Chem. Res.* **2010**, *43*, 429–439.

(18) Summers, M. A.; Buratto, S. K.; Edman, L. Morphology and Environment-Dependent Fluorescence in Blends Containing a Phenylene-vinylene-Conjugated Polymer. *Thin Solid Films* **2007**, *515*, 8412–8418.

(19) Barbara, P. F.; Gesquiere, A. J.; Park, S. J.; Lee, Y. J. Single-Molecule Spectroscopy of Conjugated Polymers. *Acc. Chem. Res.* **2005**, *38*, 602–610.

(20) Xie, Y.; Li, Y.; Xiao, L. X.; Qiao, Q. Q.; Dhakal, R.; Zhang, Z. L.; Gong, Q. H.; Galipeau, D.; Yan, X. Z. Femtosecond Time-Resolved

Fluorescence Study of P3HT/PCBM Blend Films. *J. Phys. Chem. C* **2010**, *114*, 14590–14600.

(21) Banerji, N.; Cowan, S.; Leclerc, M.; Vauthey, E.; Heeger, A. J. Exciton Formation, Relaxation, and Decay in PCDTBT. *J. Am. Chem. Soc.* **2010**, *132*, 17459–17470.

(22) Parkinson, P.; Muller, C.; Stingelin, N.; Johnston, M. B.; Herz, L. M. Role of Ultrafast Torsional Relaxation in the Emission from Polythiophene Aggregates. *J. Phys. Chem. Lett.* **2010**, *1*, 2788–2792.

(23) Piris, J.; Dykstra, T. E.; Bakulin, A. A.; van Loosdrecht, P. H. M.; Knulst, W.; Trinh, M. T.; Schins, J. M.; Siebbeles, L. D. A. Photogeneration and Ultrafast Dynamics of Excitons and Charges in P3HT/PCBM Blends. *J. Phys. Chem. C* **2009**, *113*, 14500–14506.

(24) Trotzky, S.; Hoyer, T.; Tuszynski, W.; Lienau, C.; Parisi, J. Femtosecond Up-Conversion Technique for Probing the Charge Transfer in a P3HT: PCBM Blend via Photoluminescence Quenching. *J. Phys. D: Appl. Phys.* **2009**, *42*, 055105.

(25) Westenhoff, S.; Daniel, C.; Friend, R. H.; Silva, C.; Sundstrom, V.; Yartsev, A. Exciton Migration in a Polythiophene: Probing the Spatial and Energy Domain by Line-Dipole Forster-Type Energy Transfer. *J. Chem. Phys.* **2005**, *122*, 094903.

(26) Paquin, F.; Latini, G.; Sakowicz, M.; Karsenti, P.-L.; Wang, L.; Beljonne, D.; Stingelin, N.; Silva, C. Charge Separation in Semicrystalline Polymeric Semiconductors by Photoexcitation: Is the Mechanism Intrinsic or Extrinsic? *Phys Rev. Lett.* **2011**, *106*, 197401.

(27) Labastide, J. A.; Baghgar, M.; Dujovne, I.; Venkatraman, B. H.; Ramsdell, D. C.; Venkataraman, D.; Barnes, M. D. Time- and Polarization-Resolved Photoluminescence of Individual Semicrystalline Polythiophene (P3HT) Nanoparticles. *J. Phys. Chem. Lett.* **2011**, *2*, 2089–2093.

(28) Gregory, R. B.; Zhu, Y. K. Analysis of Positron-Annihilation Lifetime Data by Numerical Laplace Inversion with the Program Contin. *Nucl. Instrum. Methods Phys. Res., Sect. A* **1990**, *290*, 172–182.

(29) Provencher, S. W. Contin — A General-Purpose Constrained Regularization Program for Inverting Noisy Linear Algebraic and Integral-Equations. *Comput. Phys. Commun.* **1982**, *27*, 229–242.

(30) Provencher, S. W. A Constrained Regularization Method for Inverting Data Represented by Linear Algebraic or Integral-Equations. *Comput. Phys. Commun.* **1982**, *27*, 213–227.

(31) Banerji, N.; Cowan, S.; Vauthey, E.; Heeger, A. J. Ultrafast Relaxation of the Poly(3-hexylthiophene) Emission Spectrum. *J. Phys. Chem. C* **2011**, *115*, 9726–9739.

(32) Vardeny, Z.; Ehrenfreund, E.; Shinar, J.; Wudl, F. Photoexcitation Spectroscopy of Polythiophene. *Phys. Rev. B* **1987**, *35*, 2498–2500.

(33) Shinar, J.; Vardeny, Z.; Ehrenfreund, E.; Brafman, O. Photoluminescence and Optically Detected Magnetic-Resonance in Polythiophene. *Synth. Met.* **1987**, *18*, 199–202.

(34) Vardeny, Z.; Ehrenfreund, E.; Brafman, O.; Nowak, M.; Schaffer, H.; Heeger, A. J.; Wudl, F. Photogeneration of Confined Soliton Pairs (Bipolarons) in Polythiophene. *Phys. Rev. Lett.* **1986**, *56*, 671–674.

(35) Guo, J.; Ohkita, H.; Benten, H.; Ito, S. Near-IR Femtosecond Transient Absorption Spectroscopy of Ultrafast Polaron and Triplet Exciton Formation in Polythiophene Films with Different Regioregularities. *J. Am. Chem. Soc.* **2009**, *131*, 16869–16880.

(36) Guo, J.; Ohkita, H.; Benten, H.; Ito, S. Charge Generation and Recombination Dynamics in Poly(3-hexylthiophene)/Fullerene Blend Films with Different Regioregularities and Morphologies. *J. Am. Chem. Soc.* **2010**, *132*, 6154–6164.

(37) Bredas, J.-L.; Norton, J. E.; Cornil, J.; V. Coropceanu, V. Molecular Understanding of Organic Solar Cells: The Challenges. *Acc. Chem. Res.* **2009**, *42*, 1691–1699.

(38) Do, K.; Huang, D. M.; Faller, R.; Moule, A. J. A Comparative MD Study of the Local Structure of Polymer Semiconductors P3HT and PBTTT. *Phys. Chem. Chem. Phys.* **2010**, *12*, 14735–14739.

(39) Moule, A. J.; Allard, S.; Kronenberg, N. M.; Tsami, A.; Scherf, U.; Meerholz, K. Effect of Polymer Nanoparticle Formation on the Efficiency of Polythiophen Based "Bulk-Heterojunction" Solar Cells. *J. Phys. Chem. C* **2008**, *112*, 12583–12589.

(40) Guskova, O. A.; Khalatur, P. G; Khokhlov, A. R. Self-Assembled Polythiophene-Based Nanostructures: Numerical Studies. *Macromol. Theory Simul.* **2009**, *18*, 219–246.

(41) Li, Z.; Zhang, X.; G. Lu, G. Electron Structure and Dynamics at Poly(3-hexylthiophene)/Fullerene Photovoltaic Heterojunctions. *Appl. Phys. Lett.* **2011**, *98*, 083303.

(42) Melis, C.; Colombo, L.; Mattoni, A. Self-Assembling of Poly-(3-hexylthiophene). *J. Phys. Chem. C* **2011**, *115*, 576–581.

(43) Eldridge, M. D.; Madden, P. A.; Frenkel, D. Entropy-Driven Formation of a Superlattice in a Hard-Sphere Binary Mixture. *Nature* **1993**, *365*, 35–37.

(44) Bartlett, P. A Model for the Freezing of Binary Colloidal Hard-Spheres. *J. Phys.: Condens. Matter* **1990**, *2*, 4979–4989.

(45) Xu, H.; Baus, M. A Density Functional-Study of Superlattice Formation in Binary Hard-Sphere Mixtures. *J. Phys.: Condens. Matter* **1992**, *4*, L663–L668.

(46) Cottin, X.; Monson, P. A. Substitutionally Ordered Solid-Solutions of Hard-Spheres. *J. Chem. Phys.* **1995**, *102*, 3354–3360.

(47) Bartlett, P.; Pusey, P. N. Freezing of Binary-Mixtures of Hard-Sphere Colloids. *Physica A* **1993**, *194*, 415–423.

(48) Bartlett, P.; Ottewill, R. H.; Pusey, P. N. Superlattice Formation in Binary-Mixtures of Hard-Sphere Colloids. *Phys. Rev. Lett.* **1992**, *68*, 3801–3804.

(49) Sanders, J. V.; Murray, M. J. Ordered Arrangements of Spheres of 2 Different Sizes in Opal. *Nature* **1978**, *275*, 201–203.

(50) O'brien, S.; Chen, Z. Y.; Moore, J.; Radtke, G.; Sirringhaus, H. Binary Nanoparticle Superlattices in the Semiconductor−Semiconductor System: CdTe and CdSe. *J. Am. Chem. Soc.* **2007**, *129*, 15702–15709.

(51) Shevchenko, E. V.; Talapin, D. V.; Murray, C. B.; O'Brien, S. Structural Characterization of Self-Assembled Multifunctional Binary Nanoparticle Superlattices. *J. Am. Chem. Soc.* **2006**, *128*, 3620–3637.

(52) Shevchenko, E. V.; Talapin, D. V.; O'Brien, S.; Murray, C. B. Polymorphism in AB(13) Nanoparticle Superlattices: An Example of Semiconductor−Metal Metamaterials. *J. Am. Chem. Soc.* **2005**, *127*, 8741–8747.

(53) Leunissen, M. E.; Christova, C. G.; Hynninen, A. P.; Royall, C. P.; Campbell, A. I.; Imhof, A.; Dijkstra, M.; van Roij, R.; van Blaaderen, A. Ionic Colloidal Crystals of Oppositely Charged Particles. *Nature* **2005**, *437*, 235–240.

(54) Bartlett, P.; Campbell, A. I. Three-Dimensional Binary Superlattices of Oppositely Charged Colloids. *Phys. Rev. Lett.* **2005**, *95*, 128302.

(55) Bartlett, P.; Warren, P. B. Reentrant Melting in Polydispersed Hard Spheres. *Phys. Rev. Lett.* **1999**, *82*, 1979–1982.

(56) Alonzo, J.; Chen, J.; Messman, J.; Yu, X.; Hong, K.; Deng, S.; Swader, O.; Dadmun, M.; Ankner, J. F.; Britt, P.; et al. Assembly and Characterization of Well-Defined High-Molecular-Weight Poly(*p*-phenylene) Polymer Brushes. *Chem. Mater.* **2011**, *23*, 4367–4374.